Journal of Alloys and Compounds 509 (2011) 2248–2251

Contents lists available at ScienceDirect

Journal of Alloys and Compounds

journal homepage: www.elsevier.com/locate/jallcom

A novel approach to quantify nitrogen distribution in nanocrystalline-amorphous alloys

R. Amini [a,b], E. Salahinejad [a,*], M.J. Hadianfard [a], E. Askari Bajestani [a], M. Sharifzadeh [c]

[a] Department of Materials Science and Engineering, School of Engineering, Shiraz University, Zand Blvd., 7134851154, Shiraz, Iran
[b] Department of Materials Science and Engineering, Shiraz University of Technology, Modarres Blvd., 3619995161, Shiraz, Iran
[c] School of Materials Science and Engineering, Nanyang Technological University, Singapore 639798, Singapore

ARTICLE INFO

Article history:
Received 12 August 2010
Received in revised form 27 October 2010
Accepted 28 October 2010
Available online 10 November 2010

Keywords:
Amorphous materials
Nanostructured materials
Mechanical alloying
X-ray diffraction
Thermal analysis

ABSTRACT

A method is introduced to estimate nitrogen partitioning in the structure of nanocrystalline-amorphous alloys, based on X-ray diffraction, thermogravimetry, and differential scanning calorimetery. The technique quantitatively determines the contribution of crystal interstitial sites, crystalline defects, and amorphous phase to nitrogen incorporation. Typically, the method shows that in Fe–18Cr–8Mn–2.5N alloy synthesized by mechanical alloying, about 4, 21 and 75 percent of nitrogen is distributed among the crystal interstitial sites, defects, and amorphous phase, respectively.

1. Introduction

It is well known that nitrogen has advantageous effects on the mechanical properties and corrosion resistance of stainless steels. Mechanical alloying (MA) has recently attracted considerable attention as a solid-state method to incorporate nitrogen in alloys. Nitrogen alloying by MA is conducted by milling under a nitrogen atmosphere or milling with nitrides under an inert gas. The generation of a high density of defects during MA increases the nitrogen solubility markedly. In the recent years, noticeable researches on MA of stainless steels under nitrogen have been reported [1–10]. It has been found that in Fe–Cr–Mn–N stainless steels processed by MA, the considerable content of an amorphous phase exists [4–10].

Regarding nitrogen distribution in the structure of mechanically alloyed Fe-based alloys, only estimating the amount of nitrogen distributed into crystal interstitial sites has been focused. It has been reported that in Fe–1.36N [11] and Fe–4.1N [12] alloys prepared by MA, 25 and 50 percent of nitrogen is entrapped into the crystal interstitial sites, respectively. On the other hand, only 4 percent of total nitrogen is distributed among crystal interstitial sites of mechanically alloyed Fe–18Cr–8Mn–2.5N stainless steel having a nanocrystalline-amorphous structure [9]. In these studies, the nitrogen supersaturation has qualitatively been attributed to preferential sites at dislocation elastic stress fields and nanograin boundaries.

This paper presents a new technique, based on X-ray diffraction, thermogravimetry, and differential scanning calorimetery, to determine the nitrogen distribution among all probable sites, particularly for mechanically alloyed Fe–Cr–Mn–N stainless steels.

2. Experimental procedures

MA of elemental Fe–18Cr–8Mn powder mixture supplied by Merck was performed under a continuous flow of high-purity nitrogen gas and under an argon atmosphere for milling durations of 24 h to 168 h. The other milling variables are similar to those reported in Refs. [4,9]. The nitrogen amount of the as-milled powders was determined by a LECO gas analyzer (Corp., St. Joseph, MI). The powder structures were characterized by X-ray diffraction (XRD) experiments (Shimadzu Lab X-6000 with Cu Kα radiation). Using TOPAS 3 software (from Bruker AXS), the XRD data were analyzed to estimate the relative phase content by the Rietveld technique and the average crystallite size by the Double-Voigt method.

The amount of nitrogen distributed in the crystal interstitial sites was estimated by the XRD analyses. Moreover, to identify the contribution of other possible sites to the nitrogen incorporation, a combined thermogravimetry and differential scanning calorimetery analysis (TGA/DSC, NETZSCH, STA 449C Jupiter) was accomplished under a flowing purified argon gas atmosphere.

3. Results and discussion

Fig. 1 shows the nitrogen content of the powders milled under nitrogen as a function of milling time. The amount of nitrogen progressively increases from 0.7 wt.% to 2.95 wt.%, when the milling

* Corresponding author. Tel.: +98 917 3879390; fax: +98 711 230 7293.
E-mail address: erfan.salahinejad@gmail.com (E. Salahinejad).

0925-8388/$ – see front matter © 2010 Elsevier B.V. All rights reserved.
doi:10.1016/j.jallcom.2010.10.194

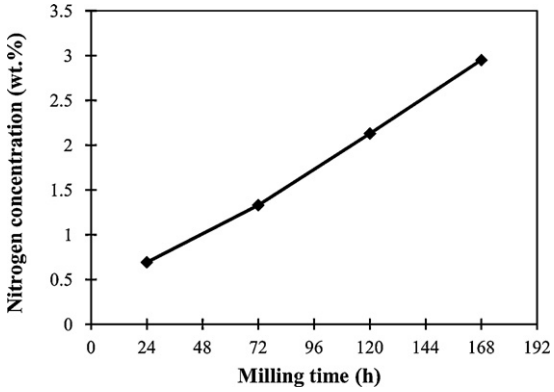

Fig. 1. Total nitrogen content of the powders milled under nitrogen.

time increases from 24 h to 168 h. In the case of milling under the nitrogen atmosphere, nitrogen adheres on virgin surfaces created during MA, dissociates, and consequently penetrates into the powders. Since the amount of structural defects generated by severe plastic deformation during milling is significantly high and since the mismatch strain of nitrogen atoms is reduced in the defects, considerable amounts of nitrogen atoms are infused to the powders, leading to the nitrogen supersaturation [1–10].

Obviously, infused nitrogen atoms are partitioned among present phases in the powders. In order to determine the type and quantity of each phase, the powder structure was evaluated by the XRD method. The results are represented in Fig. 2(a) and Table 1, revealing a combination of nanocrystalline (ferrite (α), austenite (γ)) and amorphous phases in the materials. Amorphization can be explained via high energy given to the powders during milling and

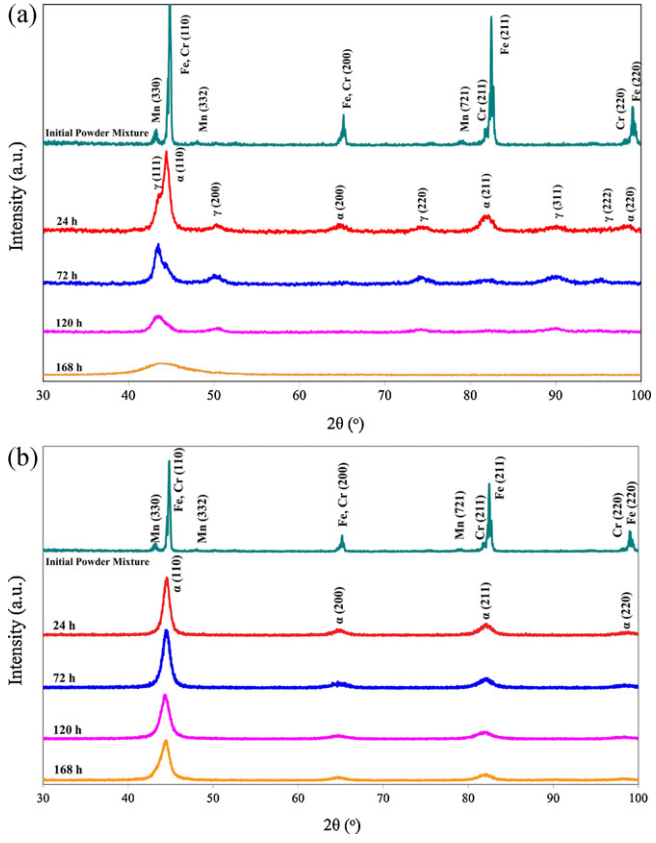

Fig. 2. XRD pattern of the powders milled under the nitrogen (a) and argon (b) atmospheres.

the effect of nitrogen on the increase in the atomic size mismatch and heat of mixing of the alloys [4–9]. The details of the calculations of the amorphous quantitative analysis by the Rietveld method have been illustrated in Ref. [4]. In addition, nanocrystallization can be argued by severe plastic deformation subjected to the powder particles in the course of milling [13]. It would be worth mentioning that the XRD results were verified by transmission electron microscopy observations [4–9].

The nitrogen infusion into the materials can be accompanied with (i) the precipitation of nitrides, (ii) the dissolution into interstitial sites of crystallites, (iii) the segregation at defects like grain boundaries and dislocations, and (iv) the distribution among interstitial sites of the amorphous phase. The contribution of all the cases to the nitrogen incorporation in the as-milled powders is assessed. Regarding the contribution of nitrides to the nitrogen partitioning, no nitride precipitate was detected in the milled powders, according to the Rietveld analyses.

The interstitial nitrogen dissolution within crystals distorts the host crystal lattice, leading to changes in interplane spacing. Accordingly, from the shift of the peaks in the XRD patterns, the content of nitrogen dissolved interstitially in the crystals can be estimated [14,15]. To take account of the influence of alloying element and milling process on the interplane spacing, the XRD analyses were also conducted on the powders milled under argon (Fig. 2(b)). Eqs. (1) and (2) yield the interstitial nitrogen contents in the nanocrystalline α-phase (N_α) and the γ-phase (N_γ), respectively [9]:

$$N_\alpha\,(\text{wt.\%}) = 36.8285\,(a_\alpha^{N}(\text{Å}) - a_\alpha^{Ar}(\text{Å})) \quad (1)$$

$$N_\gamma\,(\text{wt.\%}) = 28.5714\,(a_\gamma^{N}(\text{Å}) - 3.588) \quad (2)$$

where a_γ^{N} and a_α^{Ar} are the lattice parameter of the α-phase in the powders milled under the nitrogen and argon atmospheres; and a_γ^{N} is the lattice parameter of the γ-phase in the powders milled under the nitrogen atmosphere. Note that as austenitization does not occur in the powders milled under argon, it was not possible to calculate the austenite lattice parameter in the N-free samples [9]. Since the amount of other interstitial elements (O, C and H) in the samples milled under both the atmospheres was the same, their role in the evolution of the interplanar spacing is separated [9]. Using the relative content of the α- and γ-phases listed in Table 1 and considering the linear combination of these two phases in the interstitial nitrogen distribution, the average dissolved nitrogen content in the crystal interstitial sites (N_{int}) is obtained.

Since actual binding dislocation-interstitial energy value strongly depends on nitrogen concentration and is unknown for these materials, the theoretical prediction of interstitial nitrogen in dislocation elastic fields is not trustworthy [3]. Because of this, a novel procedure is here pointed out to estimate the contribution of the defects and amorphous phase to the nitrogen supersaturation. The approach is in accordance with the fact that heating can result in the escape of nitrogen atoms from the materials and accordingly weight losses. Because the nitrogen concentration of the powders milled under nitrogen is several orders of magnitude in excess of equilibrium contents.

Fig. 3 depicts the results of the TGA and DSC analyses of the powders milled under nitrogen. It can be observed in the TGA traces, sharp weight losses have occurred in two temperature ranges. It is noticeable that the DSC scans reveal exothermic events well in the same temperature ranges. Previous studies have implied that the first peak corresponds to the transformation of the γ-phase to α-phase and the second one is related to crystallization of the amorphous phase [4,7]. As these transformations are not essentially accompanied by any weight loss, both the weight losses are attributed to nitrogen atoms leaving the structure during heating. Indeed, these weight losses are owing to the lower nitrogen

Table 1
Results of the XRD experiments on the powders milled under nitrogen.

Milling time (h)	α-Phase percentage	γ-Phase percentage	Amorphous percentage	α-Crystallite size (nm)	γ-Crystallite size (nm)
24	51.7	19.3	29.0	18	16.2
72	17.7	38.6	43.7	11.7	11.3
120	5.3	27.3	67.4	7.8	6.1
168	–	–	100	–	–

solubility of the products compared to the parent phases. The LECO analysis of the samples heated up to the temperatures well below and above the temperature ranges confirmed the nitrogen contents in the TGA analyses.

The sample milled for 168 h having a fully amorphous structure shows no considerable weight loss in the temperature range of the first reaction. Thus, it is inferred that the first weight loss is due to the nitrogen escape from the interstitial sites and defects of the crystallites. The nitrogen content in the interstitial sites of the α-phase after the first transformation (N_{α}^{T}) can be measured by the XRD analysis of the samples heated up to the temperatures well above the reaction temperature (Eq. (1)). Subtracting N_{α}^{T} from N_{int}, the nitrogen loss from the crystal interstitial sites after the first transformation (N_{int}^{L}) is obtained. Subsequently, subtracting N_{int}^{L} from the total loss of the first event (N_{tot}^{L}) yields the loss related to defects like grain boundaries and dislocations (N_{def}^{L}).

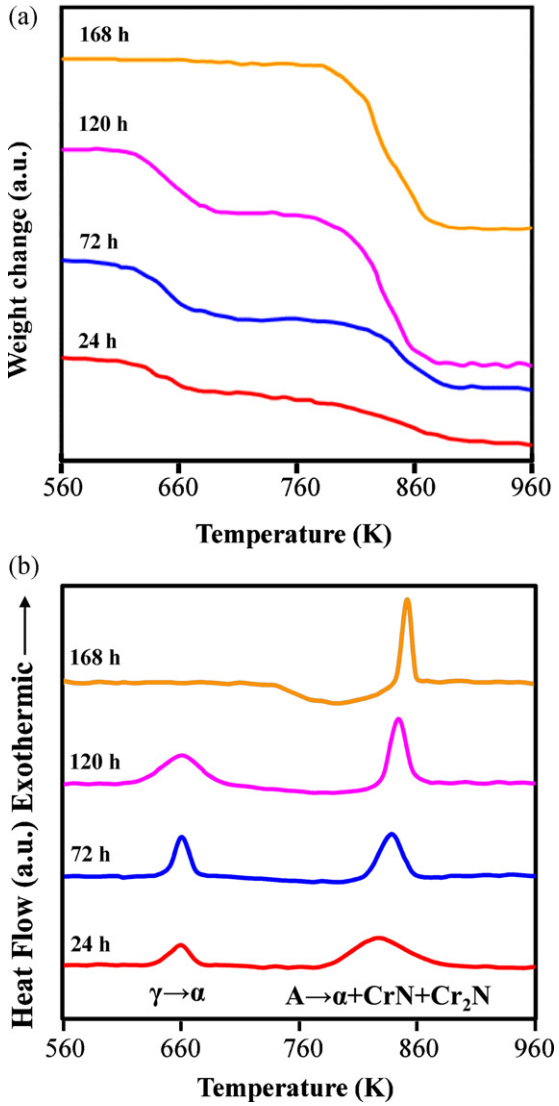

Fig. 3. TGA (a) and DSC (b) trace of the powders milled under nitrogen.

Table 2
Results of the quantitative phase analysis of the powders after crystallization.

Milling time (h)	α-Phase percentage	Cr_2N-phase percentage	CrN-phase percentage
24	99.48	0.52	0
72	99.19	0.81	0
120	98.71	1.39	0
168	97.95	1.87	0.18

The crystallization of the amorphous phase as the second transition in the thermal experiments gives rise to the development of α, CrN, and Cr_2N phases [4,7]. The related quantitative phase analysis results by the XRD method are summarized in Table 2. Subtracting the content of nitrogen in the α, CrN, and Cr_2N phases from the total nitrogen content after crystallization (N_{tot}^{F}), the final amount of nitrogen in the defects (N_{def}^{F}) can be calculated. Note that the nitrogen content in the α, CrN, and Cr_2N phases is determined by the XRD analysis, the known nitrogen content of the stoichiometric nitrides, and considering their relative contents. It is noteworthy that N_{def}^{F} consists of two parts: nitrogen contents that have existed in the defects of the as-milled powders (N_{def}^{0}) and those that have created in the defects due to crystallization (N_{def}^{C}). The fully amorphous as-milled powder has no defect ($N_{def}^{0} = 0$); consequently, N_{def}^{F} equals to N_{def}^{C} for this sample. Here, it is suggested that N_{def}^{C} for the other nanocomposite samples can be quantified by a simple proportion with respect to the amorphous phase content. In other words, the contribution of the amorphous phase to N_{def}^{F} (due to the transition to the crystals including defects) is supposed to be $N_{def}^{F} X_A$, where X_A is the weight fraction of the amorphous phase in the as-milled powders. Accordingly:

$$N_{def}^{0} = N_{def}^{F} - N_{def}^{C} = N_{def}^{F} - N_{def}^{F} X_A = N_{def}^{F} X_C \quad (3)$$

where X_C is the weight fraction of the crystalline phases, i.e. the fraction of the α-phase-plus-that of the γ-phase.

Since the weight loss in the other temperature ranges (except those of the two reactions) is negligible, the total nitrogen content in the defects of the as-milled powders (N_{def}) is calculated via adding N_{def}^{0} and N_{def}^{L}. Furthermore, subtracting $N_{int} + N_{def}$ from the total nitrogen amount of the as-milled powders gives the nitrogen content in the amorphous phase (N_A). These nitrogen contents are summarized in Table 3 for the powders milled under nitrogen. Dividing the amounts of N_{int}, N_{def}, and N_A by those of total infused nitrogen in the as-milled powders, the contribution of the crystal interstitial sites, defects, and amorphous phase to the nitrogen incorporation is identified. For instance, in the as-milled Fe–18Cr–8Mn–2.5N powder, 4, 21 and 75 percent of nitrogen is

Table 3
Nitrogen contents (wt.%) in the powders milled under nitrogen.

Milling time (h)	N_{tot}^{L}	N_{tot}^{F}	N_{int}	N_{def}	N_A
24	0.14	0.11	0.26	0.13	0.30
72	0.23	0.6	0.34	0.21	0.78
120	0.33	0.7	0.23	0.45	1.45
168	0	1.55	0	0	2.95

distributed among the crystal interstitial sites, defects, and amorphous phase, respectively. The first increase in N_{int} is because of the domination of the α-to-γ phase transformation providing larger crystal interstitial sites. Afterward, nitrogen saturation in the crystal interstitial sites is resulted and also the amorphization transition prevails. It is also noticeable that by progression of milling, the contribution of the defects and amorphous phase to the nitrogen incorporation increases. It is due to the fact that the defect density and the amorphous phase amount increase by increasing the milling time; and nitrogen atoms prefer to go to these sites to decrease the strain energy. The results indicate that the amorphous phase plays a crucial role in the nitrogen supersaturation. Eventually, it is noted that aspects of sintering and mechanical behaviors of these mechanically alloyed Cr–Mn–N stainless steels have been recently focused [16–19].

4. Conclusions

A new method was introduced to quantify nitrogen partitioning in nanocrystalline-amorphous stainless steels. The contribution of crystal interstitial sites was estimated by the XRD method from changes in interplanar spacing. The amounts of nitrogen in the defects and amorphous phase were determined by the TGA and DSC evaluations. The approach was employed for Fe–18Cr–8Mn powders milled under nitrogen gas. The results indicated that by progression of milling, the contribution of defects and amorphous phase to the nitrogen incorporation increases. In addition, the amorphous phase plays a crucial role in the nitrogen supersaturation.

References

[1] M.M. Cisneros, H.F. Lopez, H. Mancha, D. Vazquez, E. Valdes, G. Mendoza, M. Mendez, Metall. Mater. Trans. A 33 (2002) 2139–2144.
[2] M. Mendez, H. Mancha, M.M. Cisneros, G. Mendoza, J.I. Escalante, H.F. Lopez, Metall. Mater. Trans. A 33 (2002) 3273–3278.
[3] M.M. Cisneros, H.F. Lopez, H. Mancha, E. Rincon, D. Vazquez, M.J. Perez, S.D.D.L. Torre, Metall. Mater. Trans. A 36 (2005) 1309–1316.
[4] R. Amini, M.J. Hadianfard, E. Salahinejad, M. Marasi, T. Sritharan, J. Mater. Sci. 44 (2009) 136–148.
[5] R. Amini, H. Shokrollahi, E. Salahinejad, M.J. Hadianfard, M. Marasi, T. Sritharan, J. Alloys Compd. 480 (2009) 617–624.
[6] E. Salahinejad, R. Amini, M. Marasi, T. Sritharan, M.J. Hadianfard, Mater. Chem. Phys. 118 (2009) 71–75.
[7] R. Amini, E. Salahinejad, M.J. Hadianfard, M. Marasi, T. Sritharan, Mater. Sci. Eng. A 527 (2010) 1135–1142.
[8] E. Salahinejad, R. Amini, E. Askari Bajestani, M.J. Hadianfard, J. Alloys Compd. 497 (2010) 369–372.
[9] E. Salahinejad, R. Amini, M. Ghaffari, M.J. Hadianfard, J. Alloys Compd. 505 (2010) 584–587.
[10] T. Haghir, M.H. Abbasi, M.A. Golozar, M. Panjepour, Mater. Sci. Eng. A 507 (2009) 144–148.
[11] J.C. Rawers, R. Krabbe, D.C. Cook, T.H. Kim, Nanostruct. Mater. 9 (1997) 145–148.
[12] C.J. Rawers, D. Govier, R. Doan, Mater. Sci. Eng. A 22 (1996) 162–167.
[13] C. Suryanarayana, Prog. Mater. Sci. 46 (2001) 1–184.
[14] H.A. Wriedt, N.A. Gokcen, R.H. Nafziger, Bull. Alloy Phase Diagr. 8 (1987) 355–377.
[15] S. Danilkin, A. Beskrovni, E. Jadrowski, Mater. Sci. Forum 318–320 (1999) 19–24.
[16] E. Salahinejad, R. Amini, M. Marasi, M.J. Hadianfard, Mater. Des. 31 (2010) 527–532.
[17] E. Salahinejad, R. Amini, M. Marasi, M.J. Hadianfard, Mater. Des. 31 (2010) 2259–2263.
[18] E. Salahinejad, R. Amini, M.J. Hadianfard, Mater. Des. 31 (2010) 2241–2244.
[19] E. Salahinejad, R. Amini, M.J. Hadianfard, Mater. Sci. Eng. A 527 (2010) 5522–5527.